NEMESIS
Negative Effects in Medical Sciences Oral and Maxillofacial Surgery
UCL PRESSES UNIVERSITAIRES DE LOUVAIN

Artifacts related to cone beam computed tomography technology (CBCT) and their significance for clinicians: illustrated review of medical literature.

Authors:
Olszewski R DDS, MD, PhD, DrSc[1,2*]

Affiliations:

[1]Department of Oral and maxillofacial surgery, Cliniques universitaires saint Luc, UCLouvain, Brussels, Belgium
[2]Oral and maxillofacial surgery research Lab, NMSK, IREC, SSS, UCLouvain, Brussels, Belgium
*Corresponding author: Pr R. Olszewski, Department of Oral and maxillofacial surgery, Cliniques universitaires saint Luc, Université catholique de Louvain, Brussels, Belgium, phone+3227645718; fax: +3227645876;
ORCID iD:orcid.org/0000-0002-2211-7731

Disclaimer: the views expressed in the submitted article are our own and not an official position of the institution or funder.

Abstract

Objective: to explain the meaning and to illustrate technical artifacts (aliasing as well as the ring artifact) and beam hardening (metal artifact) that can be present in the dentomaxillofacial cone beam computed tomography (CBCT), and to check the accessibility of free illustrations of these artifacts in medical publications.

Material and methods: One observer applied five search equations using database PubMed. The exclusion criteria were: experimental studies, animal studies, studies not related to dentomaxillofacial area, and articles with closed access. There was no time limit for the search of articles. We limited our search to English and French language.

Results: Only 3 articles out of 434 publications were retained after application of inclusion/exclusion criteria. In these articles only 4 annotated figures were freely accessible in medical publications from PubMed.
In this paper we presented examples of aliasing, ring artifact, and beam artifacts from I-CAT, Carestream 9000 3D (Kodak), and Planmeca Promax 3D Mid CBCT. The intensity of beam hardening artifact varies from major degradation of image (i.e., subperiosteal implants, bridges, crowns, dental implants, and orthodontic fix appliances), through mean degradation (screws securing titanium mesh, head of mini-implant) to no beam hardening on metallic devices (orthodontic anchorage, orthodontic contention wire) or on dense objects (endodontic treatments, impression materials, Lego box). Some beam hardening artifacts arising from nasal piercing, hairs, or hearing aid device may be present on the image but they will not disturb the evaluation of the field of view.

Conclusions: reduction of aliasing artifact is related with the improvement of detectors quality. The presence of ring artifact means that CBCT device has lost its calibration. The field of view (FOV) needs to be reduce in order to avoid scanning regions susceptible to beam hardening (e.g., metallic restorations, dental implants). Finally, the accessibility to open knowledge on technique -related CBCT artifacts seems extremely limited when searching at PubMed database.

Keywords: CBCT, artifact, beam hardening artifact, aliasing artifact, ring artifact

Introduction

The artifact represents an abnormal signal; and this is related to the conditions in whose the measurement was performed. Technical artifacts in cone beam computed tomography (CBCT) could be due to the CBCT device (aliasing, ring artifacts) and to the cone beam interaction with metallic structures inside the dentomaxillofacial area (beam hardening artifact). Artifacts may degrade the quality of the image and this could lead to a wrong diagnosis if they are not recognized and corrected. If artifacts are very strong then image obtained may be unusable and this could results with a need to repeat the exam, which is against the radioprotection principle (ALARA-as low as reasonably achievable). Therefore, dental practitioners should be aware of existence of artifacts related to the CBCT technology and understand their source. In this study we wanted to investigate the accessibility of dental practitioners to open knowledge (open access articles) on technically related CBCT artifacts. We also wanted to explain the meaning and to illustrate diverse presentations of these artifacts for clinicians to equip them with practical knowledge to perform CBCT exams better.

Materials and methods

One observer performed the search using only PubMed database. The exclusion criteria were: experimental studies, animal studies, studies not related to dentomaxillofacial area, and articles with closed access. There was no time limit for the search of articles. We limited our search to English and French language. We performed 5 search equations from PubMed.

- First search equation was focused on accessible free full-text reviews about CBCT artifacts. The search equation was: cbct[All Fields] AND ("artifacts"[MeSH Terms] OR "artifacts"[All Fields] OR "artefact"[All Fields])) AND (Review[ptyp] AND "loattrfree full text"[sb] AND "humans"[MeSH Terms]) and was performed on 05.12.2019. We found 7 articles. After full-text reading only 2 articles were accepted for this review [1, 2];
- The aim of the second search was to find open access articles on artifacts in dentomaxillofacial CBCT from a larger perspective. Our search equation was set as: cbct[All Fields] AND ("artifacts"[MeSH Terms] OR "artifacts"[All Fields] OR "artefact"[All Fields])) AND ("humans"[MeSH Terms] AND (English[lang] OR French[lang])) and was performed on 05.12.2019. We found 390 studies. However, after title and abstract lecture there were no articles retained for further review due to the selected exclusion criteria;
- The third search equation was related to beam hardening artifact in CBCT. Our search equation was set as: (beam[All Fields] AND hardening[All

Fields] AND CBCT[All Fields]) AND "loattrfree full text"[sb]. The search was performed on 08.02.2020. We found 27 articles, and after applying exclusion criteria and after full-text reading only one article was accepted for this review [3];

- The fourth search equation was related to aliasing artifact in CBCT. Our search equation was set as: (aliasing[All Fields] AND ("artifacts"[MeSH Terms] OR "artifacts"[All Fields]) AND cbct[All Fields]) AND "loattrfree full text"[sb]. The search was performed on 08.02.2020. We found 6 articles, and after applying exclusion criteria and after full-text reading we found the same article as in third search [3];
- The fifth search equation was related to ring artifact in CBCT. Our search equation was set as: (ring[All Fields] AND ("artifacts"[MeSH Terms] OR "artifacts"[All Fields] OR "artifact"[All Fields]) AND cbct[All Fields]) AND "loattrfree full text"[sb]. The search was performed on 08.02.2020. We found 4 articles. However, after title and abstract lecture there were no articles retained for further review due to the selected exclusion criteria.

We stress the importance of 'annotated figures' (with arrows), because they bring educative value. A complex radiological image presented in the scientific article without any arrows is difficult to understand and interpret.

Results

Accessibility to open knowledge

We found only three articles [1-3] from a total of 434 articles that corresponded to our search. In the study by Pauwels et al., [1] there were no figures on artifacts available among a total number of 34 figures. In the study by Schulze et al., [2] we found only one annotated clinical figure on aliasing artifact. Nagarajappa et al., [3] review added one annotated clinical figure on aliasing artifact, one annotated clinical figure of ring artifact, and one annotated clinical figure on beam hardening.

All selected articles presented very limited pictorial results. In this article we present a wide range of artifacts (figures 1-45). All images presented below belongs to the authors database.

Aliasing artifact

For each projection the voxels close to the source will be traversed by more recorded "rays" than those close to the detector [2] because of the cone beam divergence itself [2]. This causes aliasing which represents itself as line patterns (moiré patterns), commonly diverging towards the periphery of the reconstructed volume [2]. These patterns can decrease the quality of image. They can appear in different types of dental CBCT (I-CAT, Carestream 9000 3D (Kodak)) (Figures 1, 2).

Fig. 1. I-CAT CBCT. Axial view of mandible and cervical vertebra. Thick arrows: aliasing artifacts. Dashed arrow: streaks from beam hardening artifact (metal crow on tooth n°46); thin arrow: black space between metallic elements (dental implants on mandibular left side) from beam hardening artifact.

Fig. 2. Carestream 9000 3D (Kodak). Axial view of left mandible. Arrows: Aliasing artifact visible in soft tissues around the bone.

Ring artifact

Ring artifacts are visible as concentric rings centered around the location of the axis of rotation [2]. They are most prominent when homogeneous media are imaged [2], such as soft tissues of the mouth floor. They are caused by defect or uncalibrated detector elements [2].

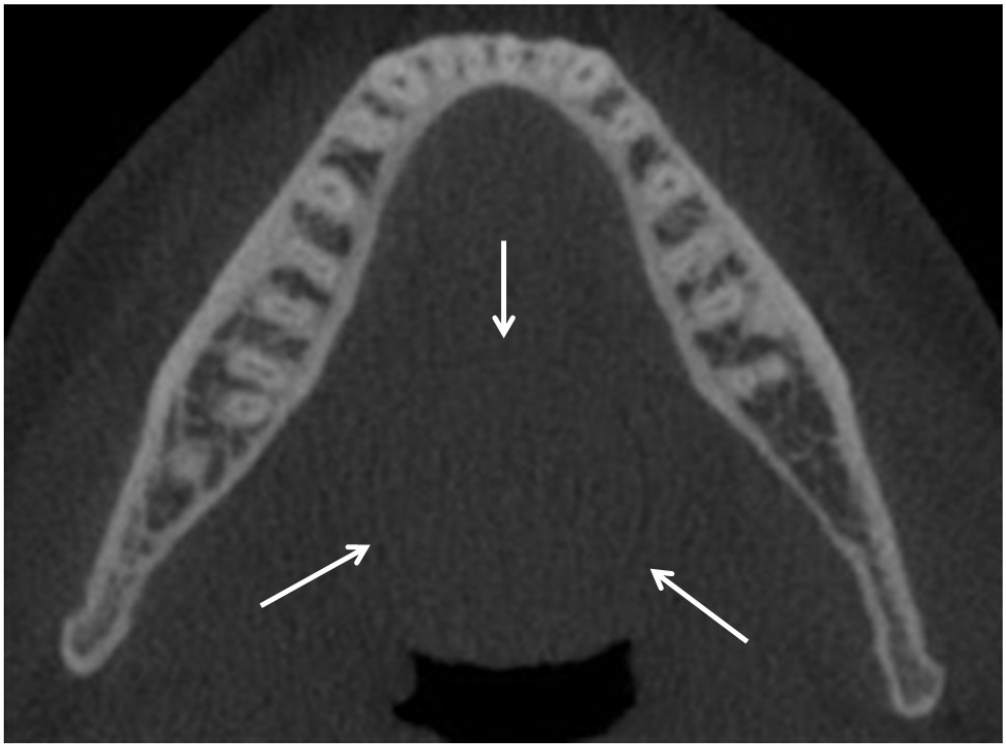

Fig. 3. I-CAT CBCT. Axial view of mandible. Arrows: ring artifact visible in the middle of mouth floor.

Beam hardening (metal)

An X-ray beam is composed of individual photons with a range of energies [3]. As the beam passes through an object, it becomes “harder,” i.e., its mean energy increases, because the lower-energy photons are absorbed more rapidly than the higher-energy photons [3-5] Highly absorbing materials such as metal (amalgam filling, dental implants) [3, 4] function as a filter positioned within the object [3]. Beam hardening artifacts are influenced by object density ([6]. If the emitted spectrum contains more relatively lower-energetic rays than that recorded on the detector (i.e. the beam is hardened), a non-linear error (relatively too much energy recorded in the beam path behind highly absorbing materials) is induced in the recorded data [3]. In the 3D reconstruction, the error is back projected into the volume, resulting in darks streaks.[4]. Because the CBCT X-ray beam is heterochromatic and has lower mean kilovolt (peak) energy compared with conventional CT, this artifact is more pronounced on CBCT images [3]. These can be reduced using iterative reconstruction [3]. Beam hardening artifact results in dark bands or streaks between dense objects in the image [3] (Figures 5, 8, 9, 10, 11, 14, 15). This artifact is related to the presence of dental amalgam (Figures 4, 5), to crowns and bridges (Figure 6-8), and to dental implants (Figure 9).

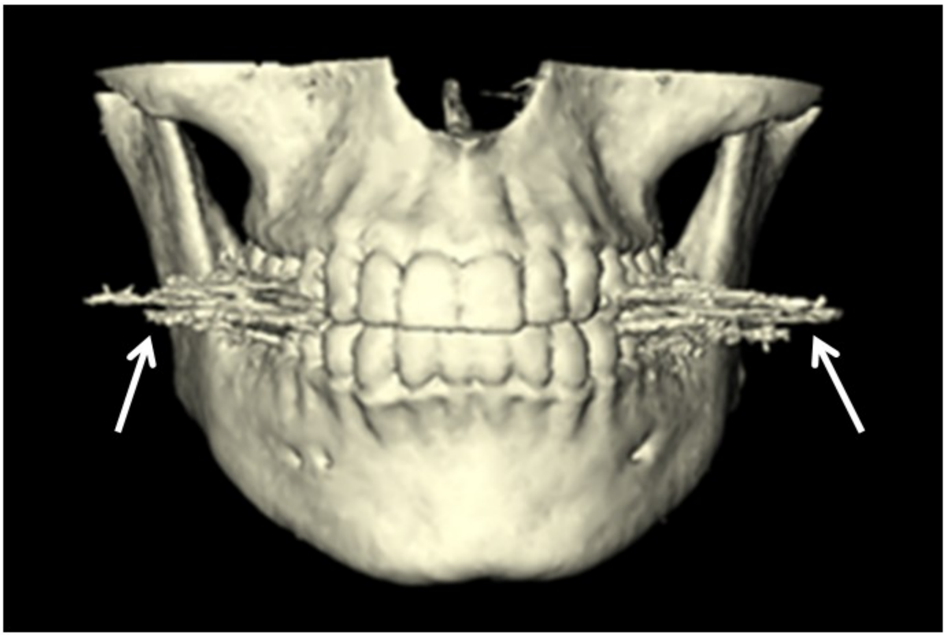

Fig. 4. I-CAT CBCT. 3D reconstruction of mandible and maxilla. Arrows: 3D reconstruction of streaks artifacts because of beam hardening from dental amalgam fillings.

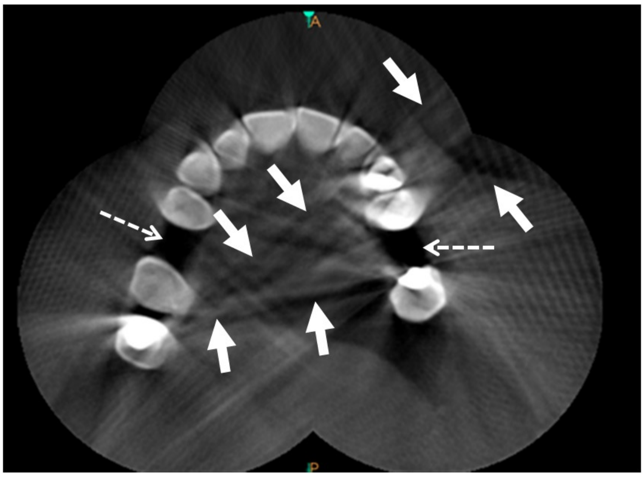

Fig. 5. Carestream 9000 3D (Kodak). Axial view of upper maxilla. Fusion of three fields of view of axial view. Thick arrows: complex pattern of streaks from beam hardening artifact due to metallic fillings on teeth n°17, 23, 24, and 26 (dental amalgam). Dashed arrows: dark stripes between dense objects in the image (beam hardening artifact).

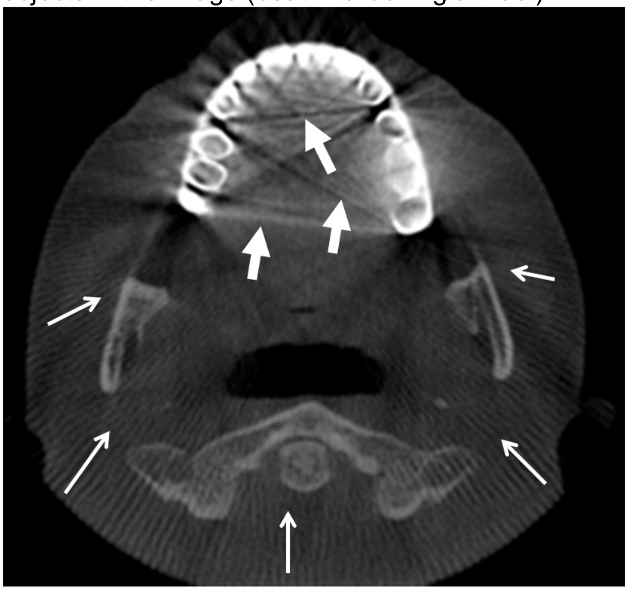

Fig. 6. I-CAT CBCT. Axial view of mandible and of cervical spine. Thick arrows: complex pattern of streaks due to crowns and bridge present on all upper teeth. Thin arrows: aliasing artifact.

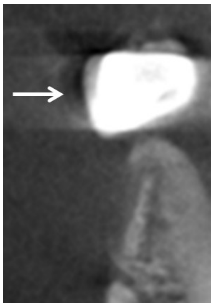

Fig. 7. I-CAT CBCT. Frontal view of mandible and of intermediary element of a bridge. Arrow: streak artefacting only a horizontal space around the metallic element. There exists no vertical streak due to beam hardening.

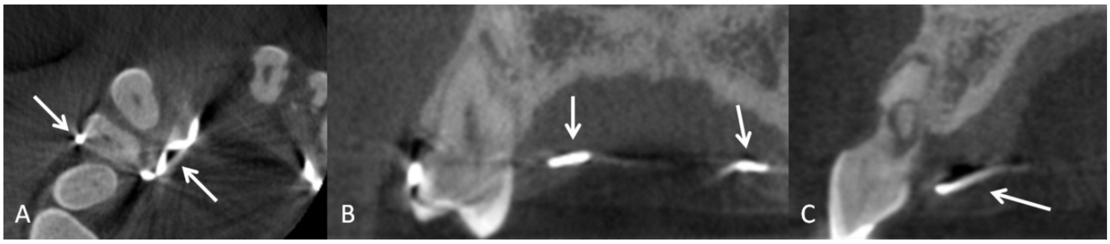

Fig. 8. Carestream 9000 3D (Kodak). Maxilla. A. Axial view. B. Frontal view. C. Sagittal view. Arrows showing hooks of removable partial prosthesis. Presence of streaks and black stripes due to beam hardening from metallic element.

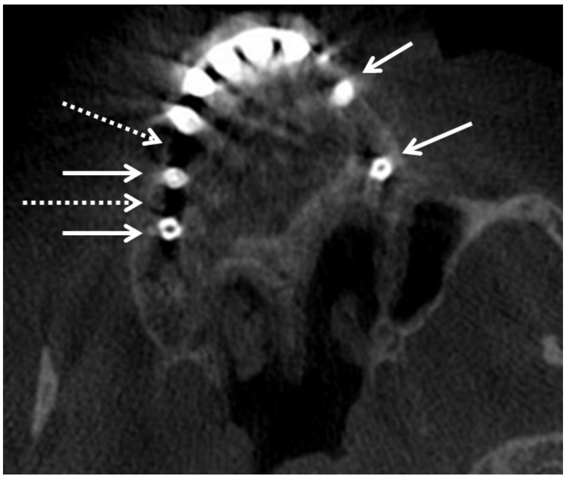

Fig. 9. I-CAT CBCT. Axial view of maxilla. Thin arrows: Beam hardening around implants. Dashed arrows: dark stripes due to beam hardening between dense objects.

Especially, superiosteal implants [7] show massive beam hardening artifact making impossible the evaluation of adjacent soft and hard tissues (Figures 10-13).

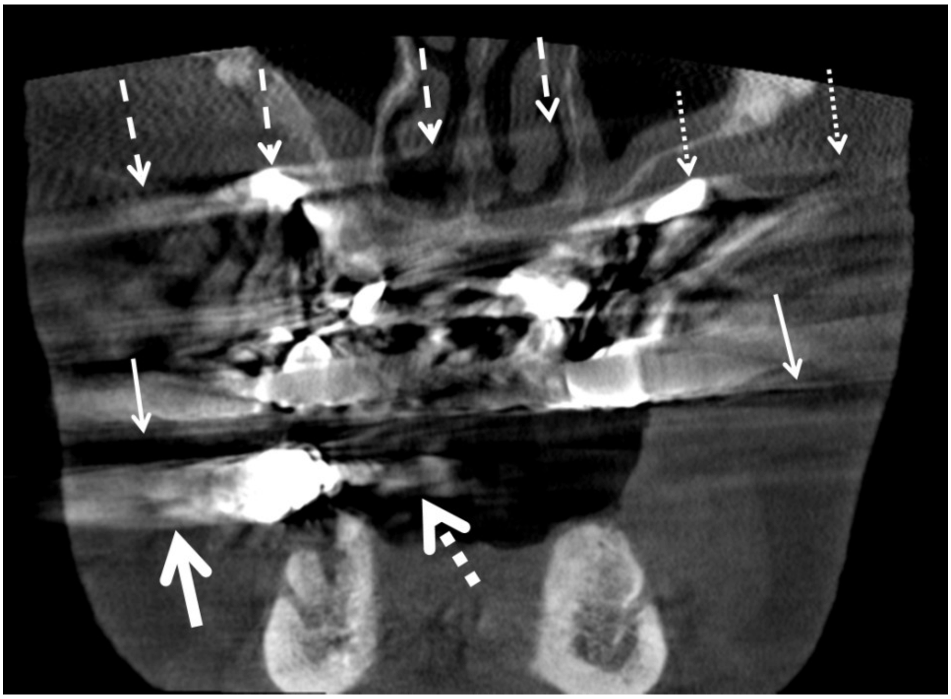

Fig. 10. Planmeca Promax 3D Mid. Frontal view of maxilla and mandible. Dashed arrows: upper limit of metallic artifacts from right side. Superimposition of artifact on right vestibular soft tissue, on right maxillary sinus, and on nasal fossae. Thin dashed arrows: upper limit of metallic artifact from left side. Superimposition of artifact on left vestibular soft tissue. Metallic artifacts are related to subperiosteal implants. Thin arrows: lower limit of metallic artifact that are related to the bridge. Thick arrow: metallic artifact related to the right mandibular bridge. Important superimposition of artifact on right vestibular soft tissue. Thick dashed arrow: metallic artifact related to the mandibular bridge. Few superimposition of metallic artifact on lingual side.

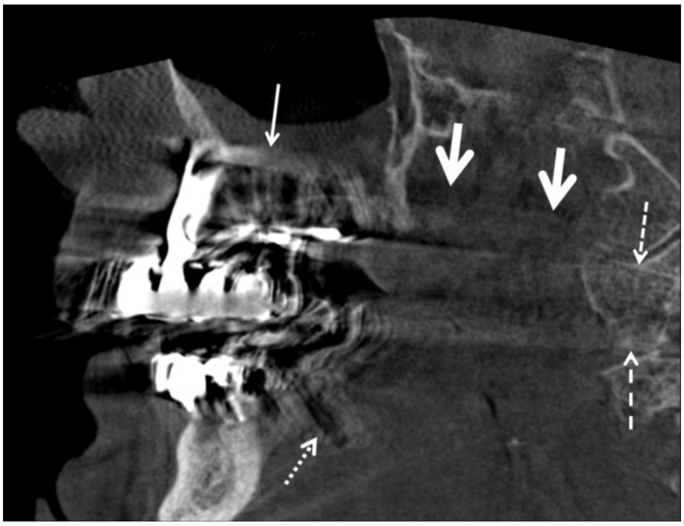

Fig. 11. Planmeca Promax 3D Mid. Sagittal view of maxilla and mandible. Thin arrow: superimposition of metallic artifact from subperiosteal implants on the floor of maxillary sinus. Thick arrows: metallic artifact from subperiosteal implants superimposed on nasopharyngeal space. Thin dashed arrows: metallic artifact from subperiosteal implants superimposed on cervical spine. Thin punctiform arrow: beam hardening from mandibular dental implant.

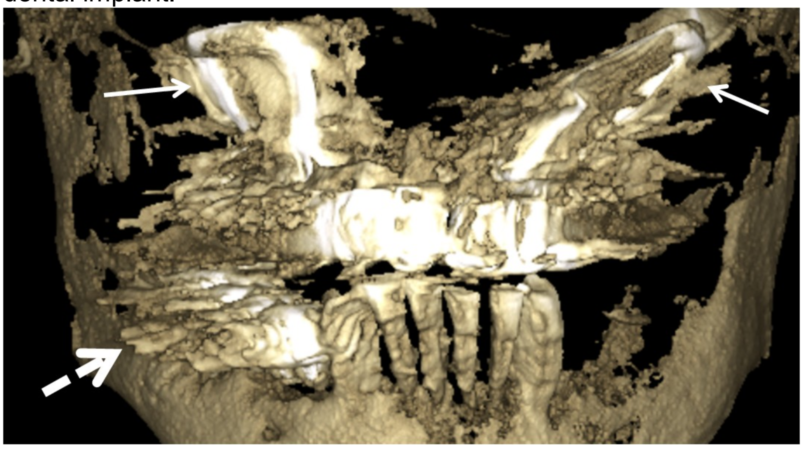

Fig. 12. Planmeca Promax 3D Mid. Anterior view of 3D reconstruction of maxilla and mandible. Thin arrows: metallic artifacts related to subperiosteal implants. Thick dashed arrow: massive metallic artifact related to right mandibular bridge.

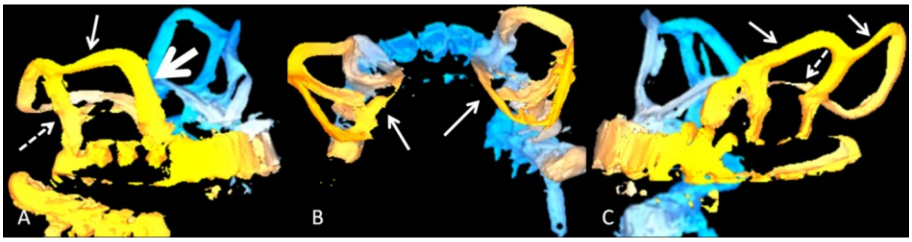

Fig. 13. Planmeca Promax 3D Mid. 3D reconstruction of subperiosteal implant. A. Right lateral view. Thick arrow: right vestibular anterior pillar. Thin arrow: vestibular horizontal bar. Thin dashed arrow: right vestibular posterior pillar. B. Posterior view. Arrows: subperiosteal implant on palatal side. C. Left lateral view. Thin arrows: left vestibular horizontal bars. Thin dashed arrow: reinforcement bar on left palatal side.

Beam hardening artifact is also related to the orthodontic fix appliances (Figure 14), palatal expansion devices (Figure 15), and to orthodontic crowns (Figure 16).

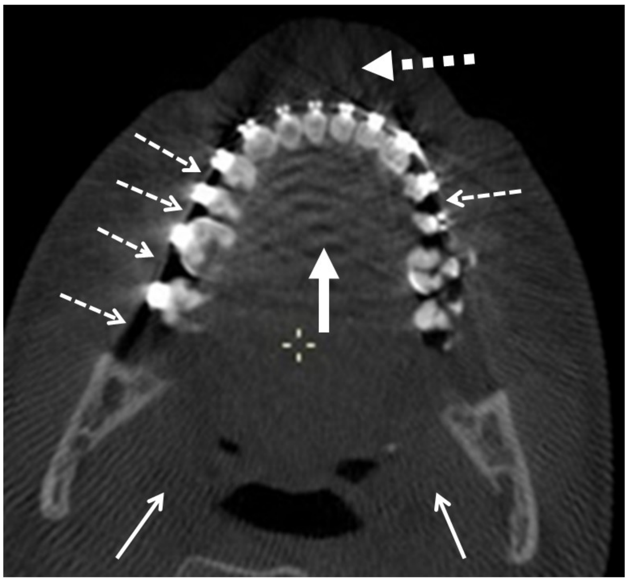

Fig. 14. I-CAT CBCT. Axial view of mandible and orthodontic treatment, vestibular brackets, and wire. Thick dashed arrow: complex pattern of streaks (metallic artifacts) in vestibular area. Thick arrow: complex pattern of streaks (metallic artifacts) on lingual side. Thin dashed arrows: dark spaces due to beam hardening of adjacent brackets. Thin arrows: aliasing artifact.

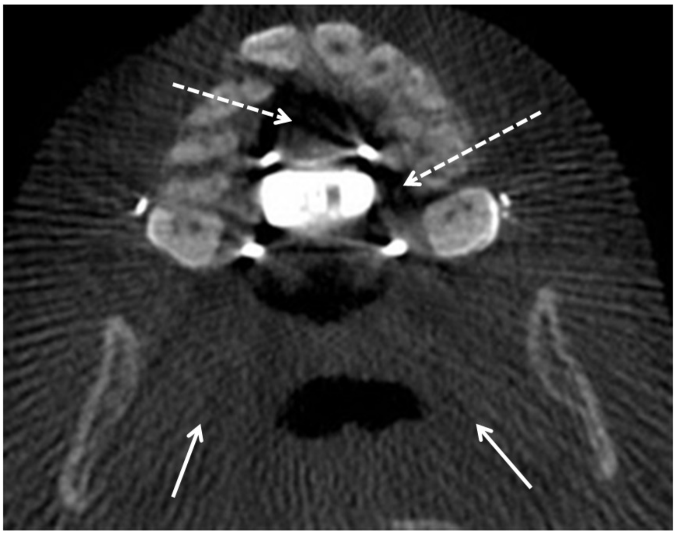

Fig. 15. I-CAT CBCT. Axial view of maxillary bone. Thin dashed arrows: massive metallic artifacts around a palatal expansion device. Thin arrows: aliasing artifacts.

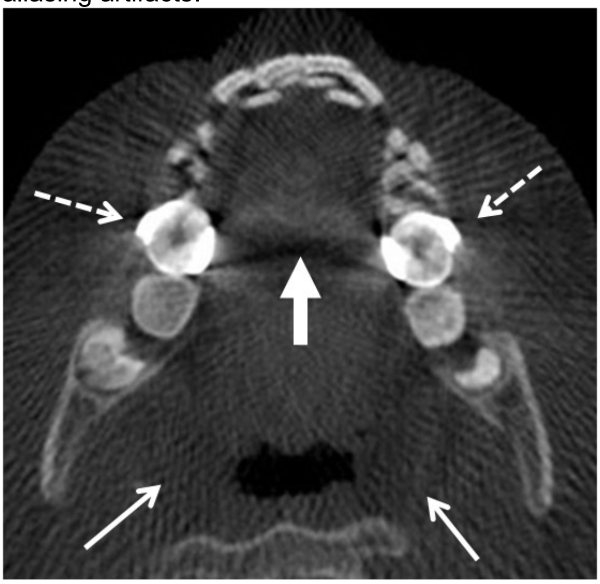

Fig. 16. I-CAT CBCT. Axial view of the mandible. Dashed arrows: orthodontic crowns on teeth n°36, and n°46. Thick arrow: Additive effect of streak artifact from two orthodontic crowns. Thin arrows: aliasing artifact.

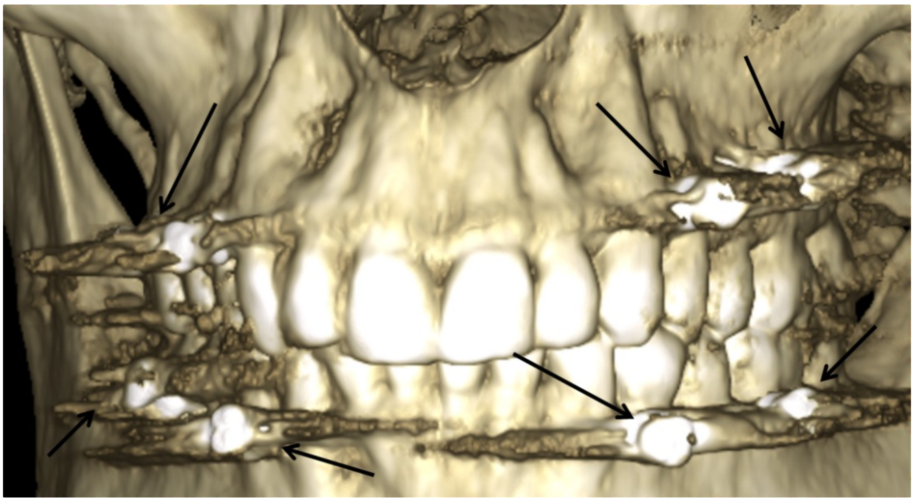

Fig. 17. Planmeca Promax 3D Mid. Anterior view of 3D reconstruction of maxilla and mandible. Black arrows: intermaxillary fixation screws presenting important beam hardening artifact.

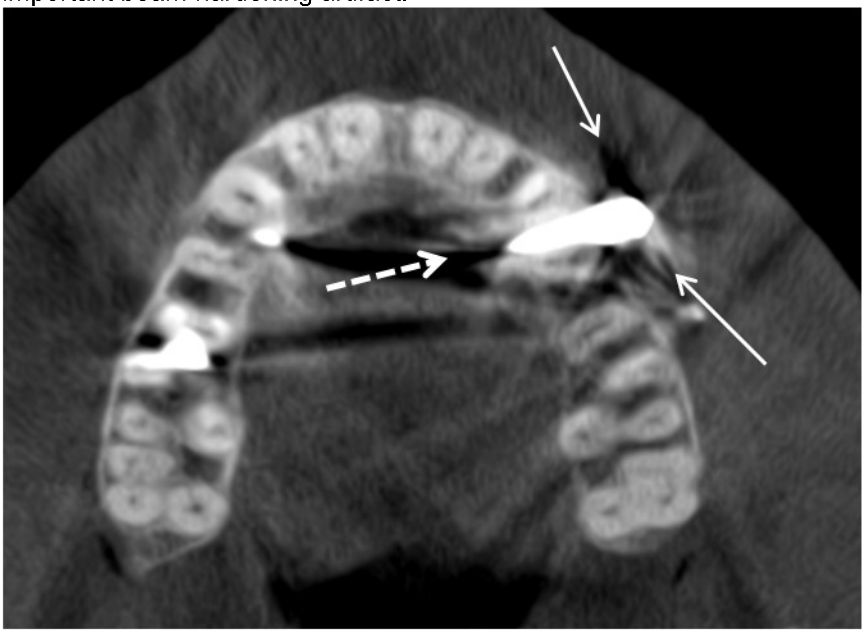

Fig. 18. Planmeca Promax 3D Mid. Axial view of the maxilla. Arrows: important beam hardening artifact around the head of intermaxillary fixation screw. Dashed arrow: black stripe along the long axis of the screw.

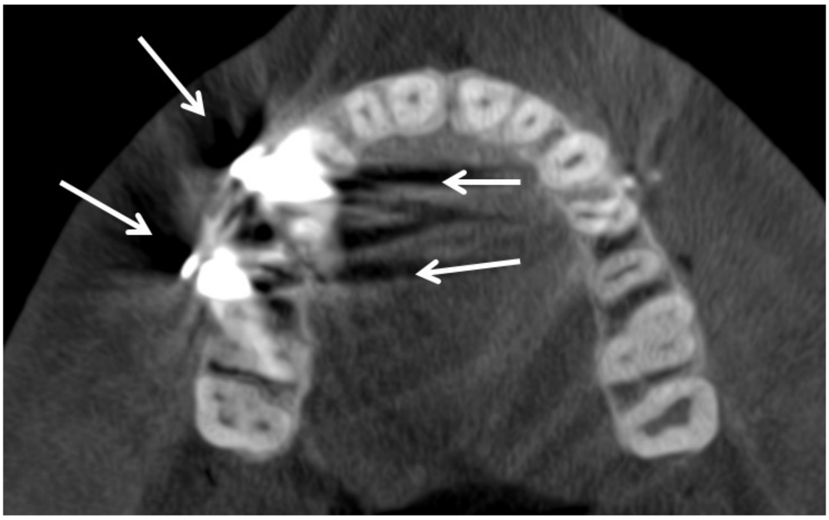

Fig. 19. Planmeca Promax 3D Mid. Axial view of the maxilla. Arrows: important beam hardening artifact around the head of intermaxillary fixation screw with creation of black spaces in vestibular soft tissues surrounding the screw. Presence of black stripes along the long axis of screws. Impossibility to evaluate the area between screw and dental roots.

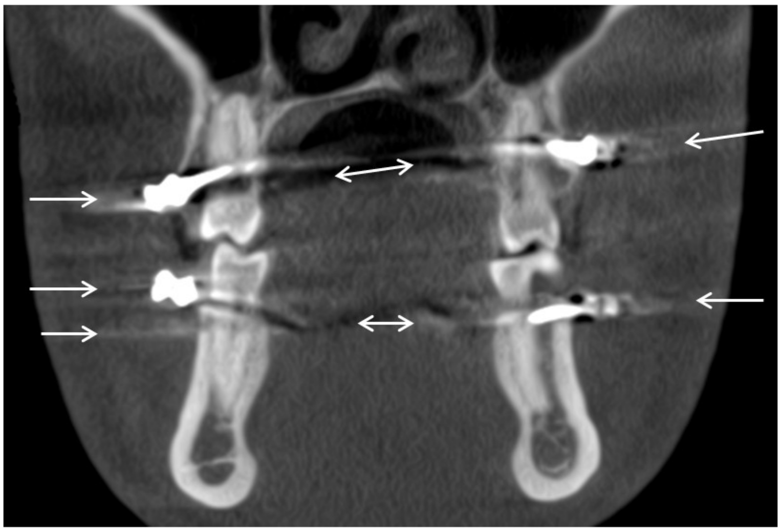

Fig. 20. Planmeca Promax 3D Mid. Frontal view of maxilla and mandible. Arrows: stripes in soft tissue around intermaxillary fixation screws due to beam hardening artifact. Double arrows: cumulation of black stripes from screws positioned at the same level on the right and the left side.

Some metallic elements present in the field of view may show a beam hardening artifact, however this artifact will not disturb the evaluation of dentomaxillofacial structures. Nasal piercings (Figure 21), hearing aid devices (Figures 22, 23), and metallic clips on dreadlocks (Figures 24-27) give beam hardening artifacts with streaks present outside of the dentomaxillofacial area.

Fig. 21. I-CAT CBCT. Axial view of maxilla. A. Arrow: piercing in left nostril wing with metallic beam hardening artifact. B. Arrow: ring of piercing in left nostril wing with metallic beam hardening artifact.

Hearing aid device (Figures 22, 23) shows beam hardening streaks and dark space between the device and temporal bone, and streaks are present around the device and are superimposed on the skull image.

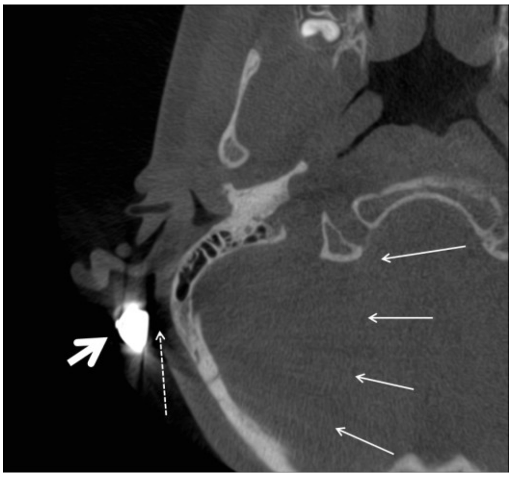

Fig. 22. Planmeca Promax 3D Mid. Axial view of external ear and right side of the skull. Thick arrow: hearing aid device with massive beam hardening artifact. Dashed arrow: black hole artifact close to the hearing aid device. Arrows: beam hardening artifact causing streaks superimposed on the image of the skull.

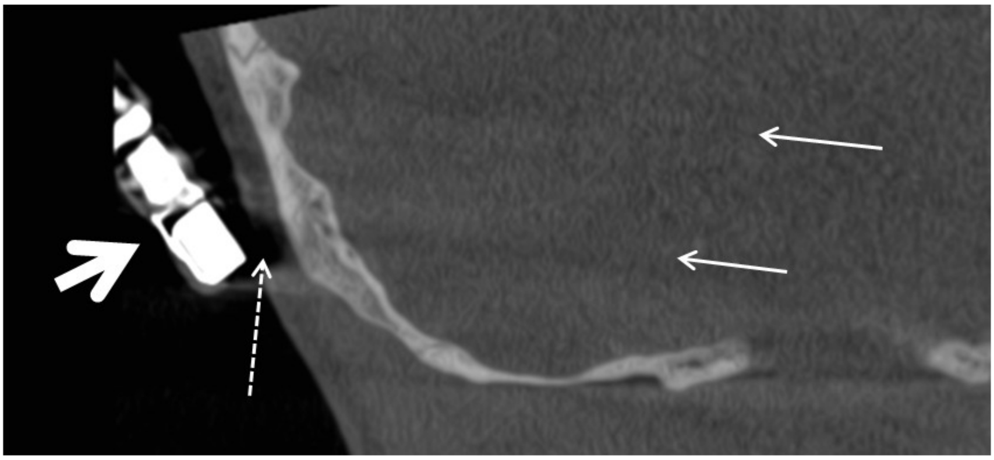

Fig. 23. Planmeca Promax 3D Mid. Sagittal view of right external ear area and of the right side of the skull. Thick arrow: hearing aid device. Dashed arrow: black hole artifact close to the hearing aid device. Arrows: beam hardening artifact causing stripes superimposed on the image of the skull.

Fig. 24. Planmeca Promax 3D Mid. Frontal view of 3D reconstruction of mandible, maxilla, soft tissues, and hair (blue). Arrows: metallic clips on hair dreadlocks.

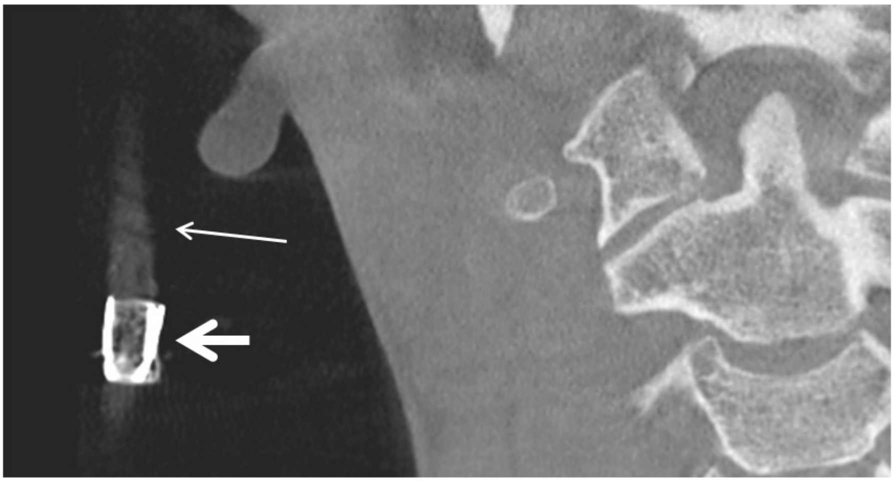

Fig. 25. Planmeca Promax 3D Mid. Frontal view of right neck area. Thick arrow: metallic clip around hair dreadlock. Thin arrow: hair dreadlock.

Fig. 26. Planmeca Promax 3D Mid. Axial view of right neck area. Arrows: beam hardening artifact from metallic clip on the dreadlock.

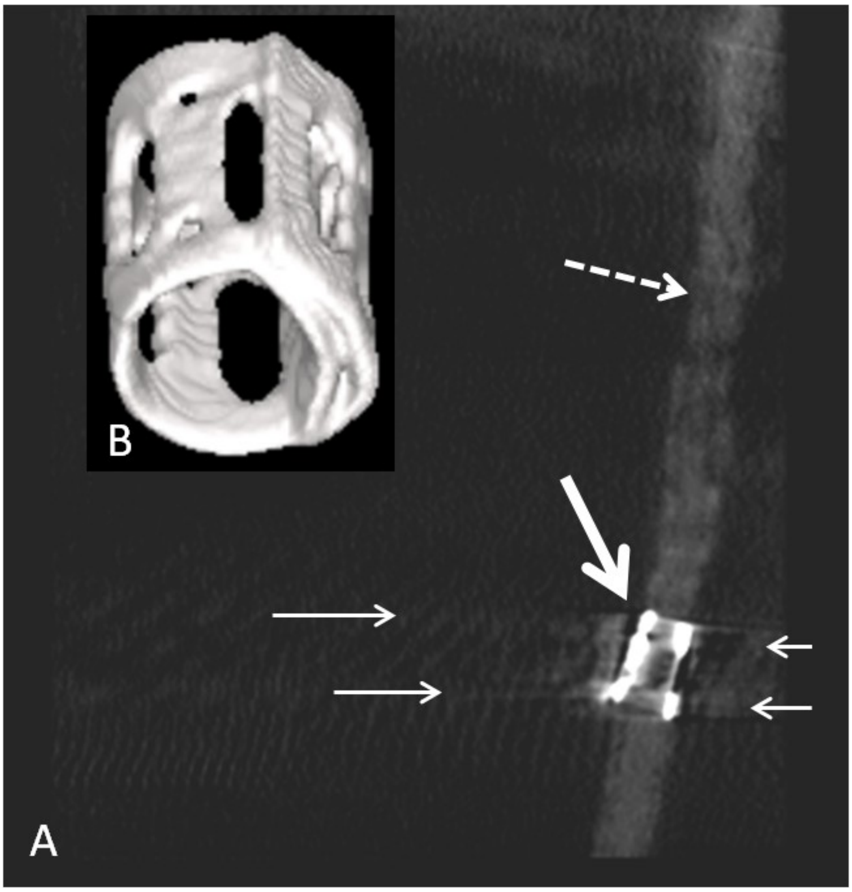

Fig. 27. Planmeca Promax 3D Mid. A. Frontal view of a dreadlock. Thick arrow: metallic clip. Thin arrows: beam hardening artifact around the metallic clip. Dashed arrow: hair dreadlock. B. The 3D reconstruction of the metallic clip.

Osteosynthesis titanium orbital plates present few beam hardening artifacts giving streaks around the plate (Figures 28-30). Osteosynthesis titanium mesh provides very few beam hardening artifacts that are visible only on 2D slices (Figures 32, 33) and not present on 3D reconstruction (Figure 31). However, screws securing titanium orbital plates (Figure 29) and mesh (Figure 33) show beam hardening artifacts with presence of streaks arising in all directions around the head of the screw (Figure 29) and along the long axis of the screw (Figure 33).

Osteosynthesis plates show few beam hardening artifacts that are visible only on 2D slices (Figure 35) and not present on 3D reconstruction (Figure 34).

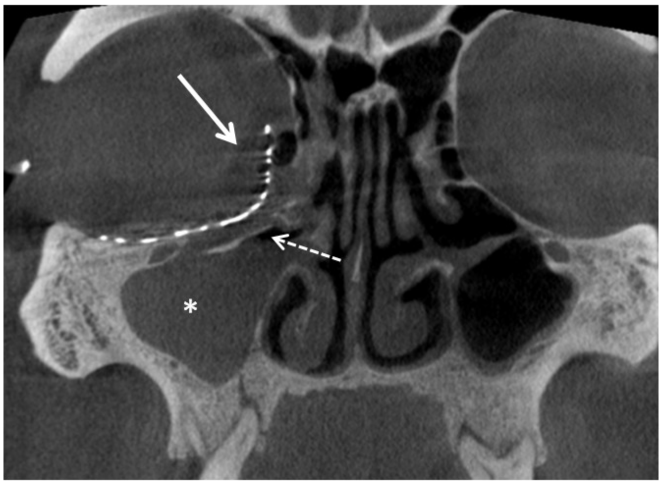

Fig. 28. Planmeca Promax 3D Mid. Frontal view of the maxilla and of the orbits. Thin arrow: prebended titanium mesh for reconstruction of the floor and of the medial wall of the right orbit. Metallic artifacts from the titanium mesh and present on the right side of the mesh. Thin dashed arrow: fractured orbital bone floor fallen inside the right maxillary sinus; *massive thickening of the right maxillary sinus mucosa.

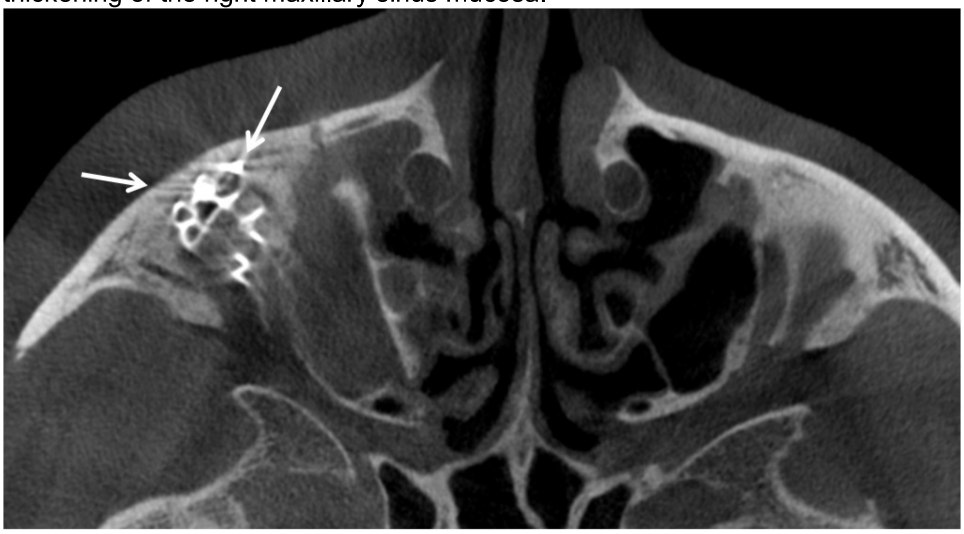

Fig. 29. Planmeca Promax 3D Mid. Axial view of orbital floor. Arrows: metallic artifacts from screws positioned on the right lower orbital rim to hold the titanium mesh in place.

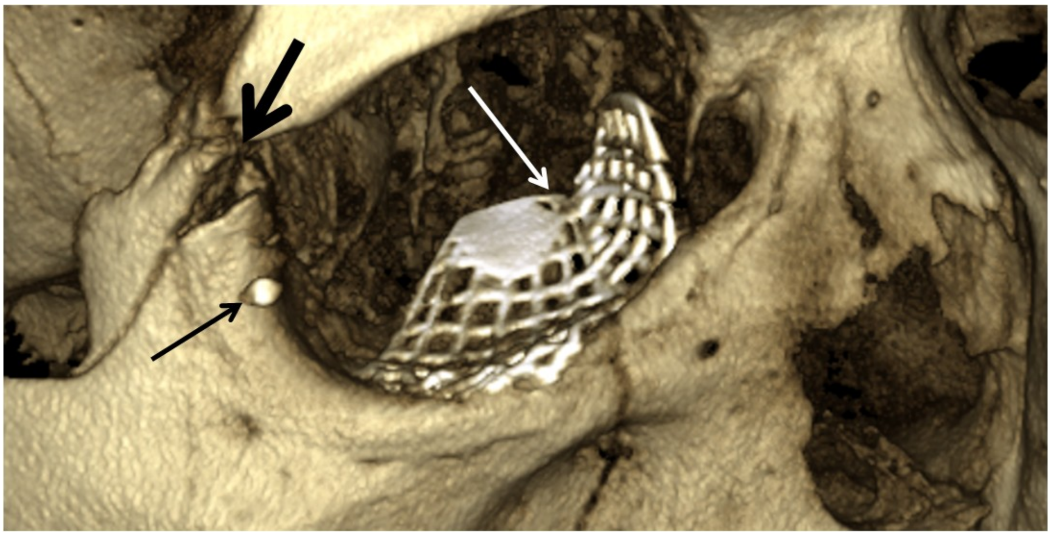

Fig. 30. Planmeca Promax 3D mid. Anterior and right lateral view of the 3D reconstruction of the right orbit. White arrow: prebended titanium mesh. Black thin arrow: subcutaneous dense foreign body without metallic artifact (plastic?). Black thick arrow: complex fracture at the right frontozygomatic junction.

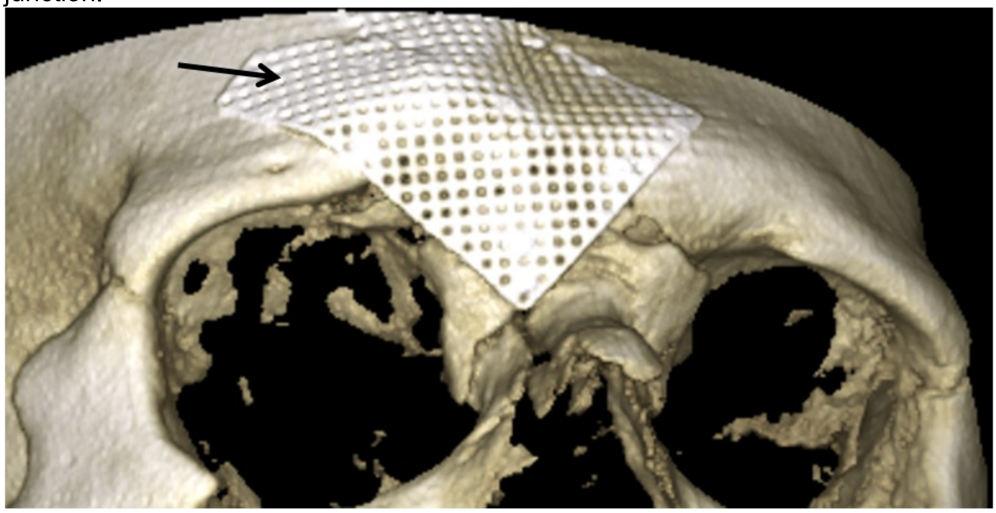

Fig. 31. Planmeca Promax 3D mid. Frontal view of the 3D reconstruction of frontal bone and of orbital roof. Titanium mesh fixing frontal and nasal fractures. No presence of metallic artifact.

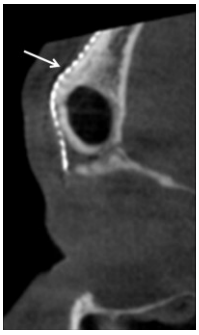

Fig. 32. Planmeca Promax 3D mid. Sagittal view of frontal sinus. Arrow: titanium mesh without metallic artifact.

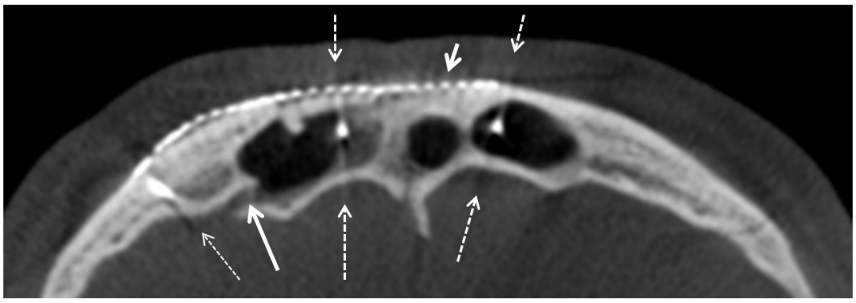

Fig. 33. Planmeca Promax 3D mid. Axial view of frontal sinus. Short arrow: mild metallic artifact from titanium mesh superimposed on surrounding soft and bone tissue. Dashed arrows: metallic artifacts stripes from screws fixing the titanium mesh on the frontal bone. Long arrow: fracture of the right posterior wall of the frontal sinus.

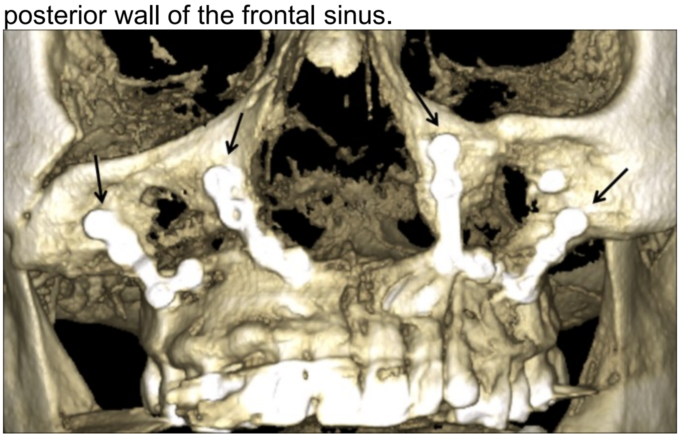

Fig. 34. Planmeca Promax 3D mid. Anterior view of the 3D reconstruction of the maxilla. Black arrows: titanium osteosynthesis plates without metallic artifacts.

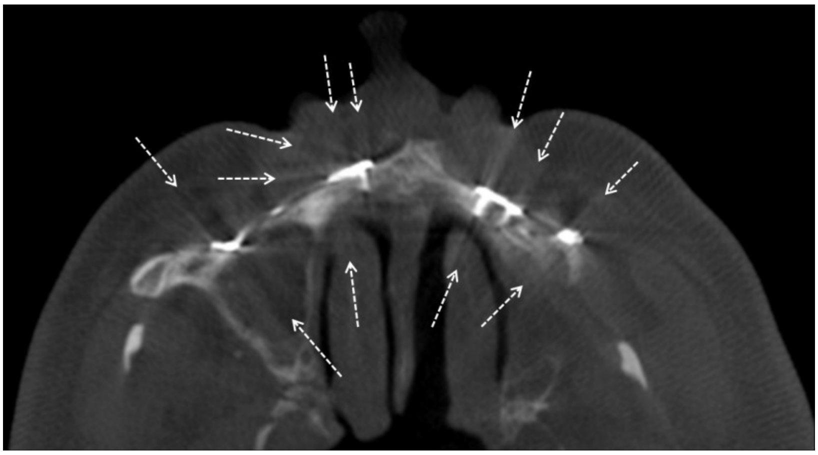

Fig. 35. Planmeca Promax 3D mid. Axial view of the maxilla. Dashed arrows: metallic artifacts stripes related to beam hardening from screws fixing osteosynthesis plates to the maxilla.

Orthodontic mini-implant shows beam hardening artifact around the head of mini-implant and minor metallic artifact along the long axis of mini-implant (Figure 36).

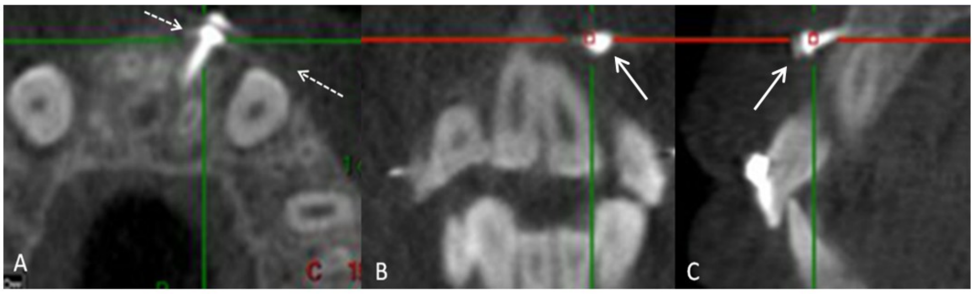

Fig. 36. I-CAT CBCT. Orthodontic mini-implant. A. Axial view of the maxilla; dashed arrows: metallic artifacts stripes from, and around the head of the implant. B. Frontal view of the maxilla; arrow: mild metallic artifacts stripes from the head of the implant. C. Sagittal view of the maxilla; arrow: mild metallic artifacts stripes from the head of the implant.

Some currently used dental elements such as composite fillings (Figure 37), endodontic filling with gutta-percha (Figures 38-40), prosthetic trays (Figure 41), orthodontic contention wire (Figure 42), pediatric crown (Figure 43), and orthodontic anchorage (Bollard type) and associated screws (Figures 44, 45) do not show beam hardening artifact.

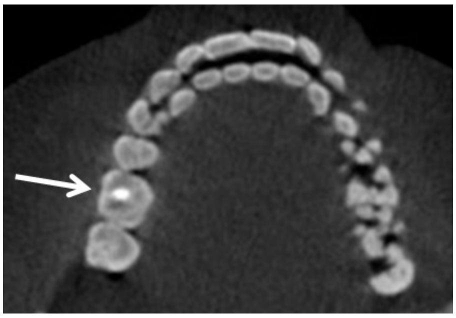

Fig. 37. I-CAT CBCT. Axial view of the maxilla. Arrow: composite filling on tooth n°16, without beam hardening artifact.

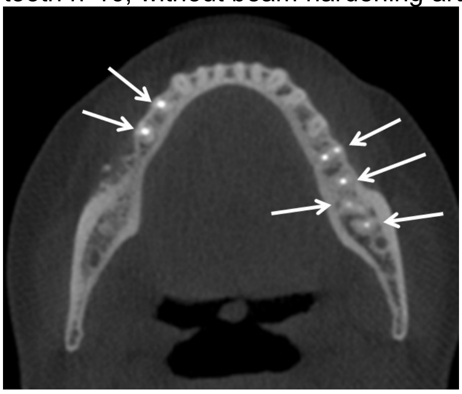

Fig. 38. I-CAT CBCT. Axial view of the mandible. Roots canals sealing with gutta-percha in roots canals of teeth n°45, 44, 36 (2 canals in mesial root),and in tooth n°37. No presence of beam hardening artifact.

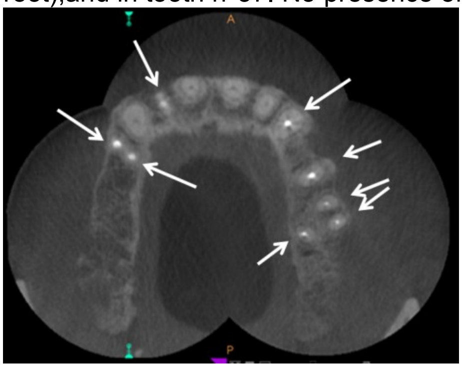

Fig. 39. Carestream 9000 3D (Kodak). Axial view of the maxilla; fusion of three fields of view. Roots canals sealing with gutta-percha in teeth n°14 (2 roots and 2 canals), 12, 23, 25, 26 (3 roots and 3 canals).

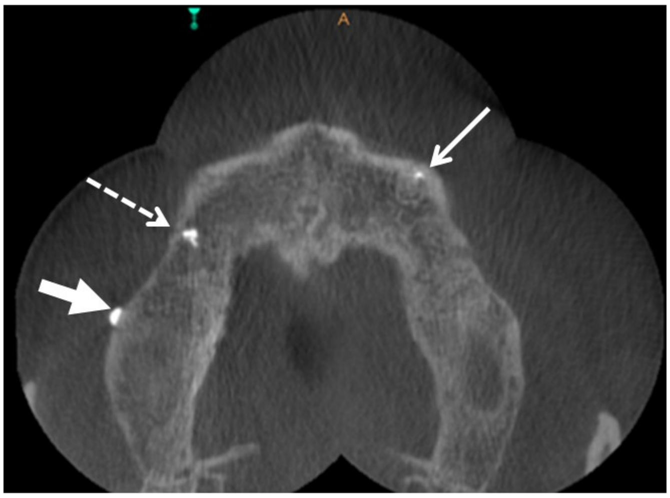

Fig. 40. Carestream 9000 3D (Kodak). Axial view of the maxilla; fusion of three fields of view. Thin arrow: root canal sealing with gutta-percha in tooth n°23. Dashed arrow: intraosseous endodontic material. Thick arrow: migration of endodontic material in subperiosteal space.

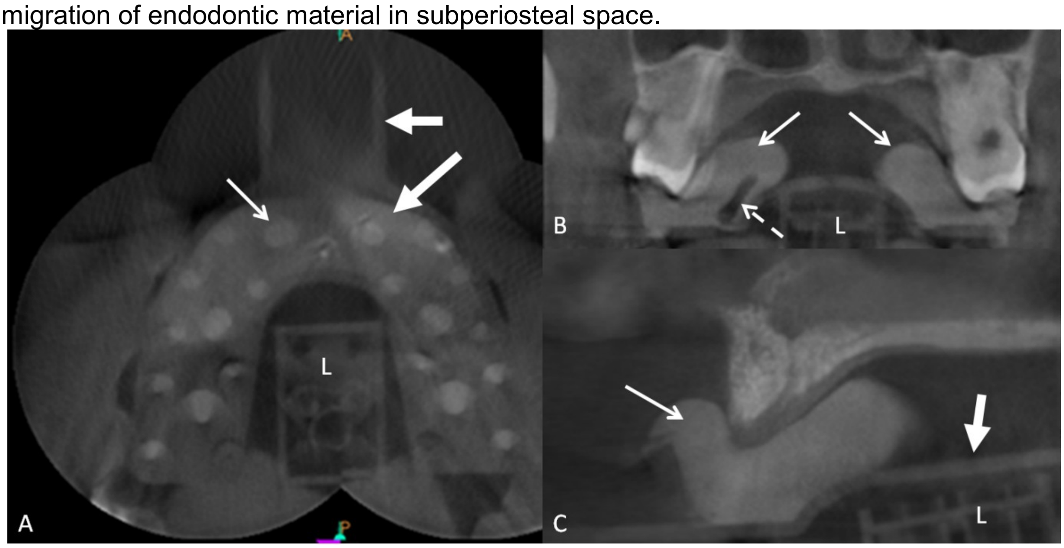

Fig. 41. Carestream 9000 3D (Kodak). A. axial view of the maxilla from a fusion of three fields of view; Thick arrows: plastic tray. Small thin arrow: dental impression material. B. Frontal view; small arrows: dental impression material. Dashed arrow: air bubble inside the dental impression material. C. Sagittal view; thick arrow: plastic tray; small arrow: dental impression material. L: lego box.

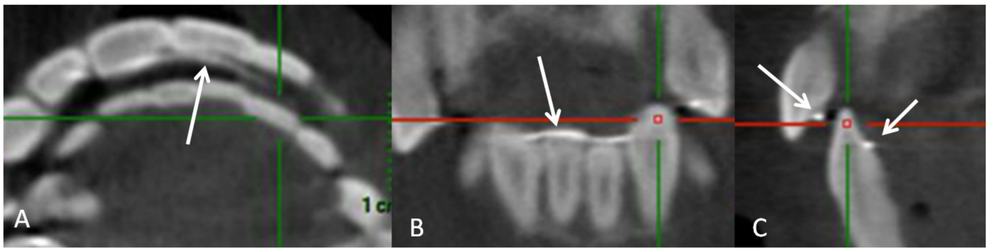

Fig. 42. I-CAT CBCT. Mandible and maxilla. A. Axial view; arrow showing upper orthodontic contention wire. B. Frontal view; arrow showing lower orthodontic contention wire. C. Sagittal view; arrows showing upper and lower orthodontic contention wires without any beam hardening artifact.

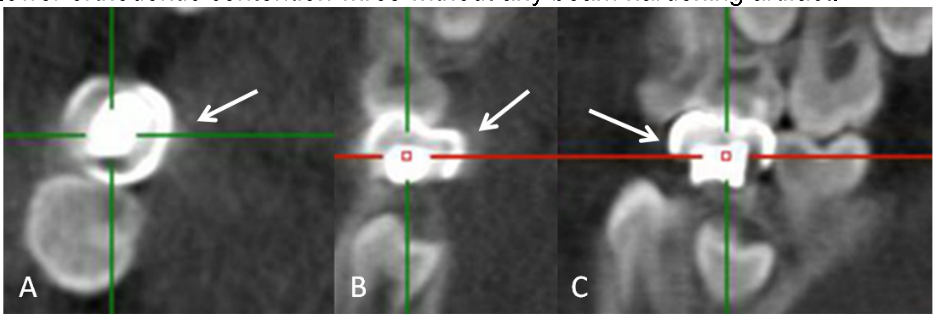

Fig. 43. I-CAT CBCT. Pediatric crown on the mandible. A. Axial view; arrow: minor streak artifact around pediatric crown on deciduous tooth. B. Frontal view; arrow: minor streak artifact around pediatric crown on deciduous tooth. C. Sagittal view; arrow: no streak artifact around pediatric crown on deciduous tooth.

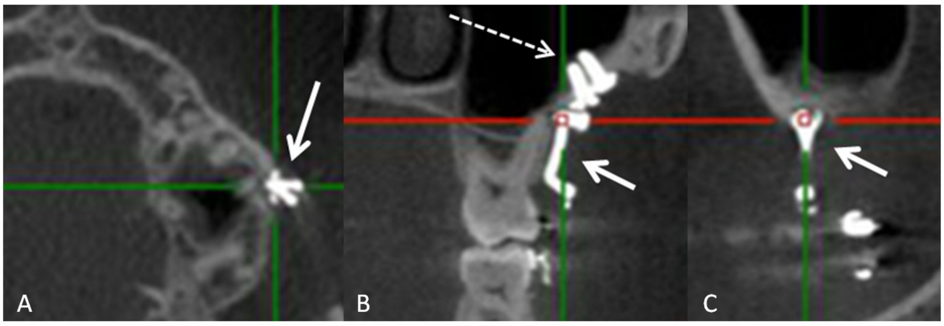

Fig. 44. I-CAT CBCT. Orthodontic anchorage plate (Bollard type). A. Axial view, arrow: mild metallic artifact on the head of a screw fixing the anchorage plate. B. Frontal view; arrow: no metallic artifact on the anchorage plate. Dashed arrow: no metallic artifact on screws fixing the anchorage plate to the maxillary bone. Lower screw close to the vestibular molar root. C. Sagittal view; arrow: no metallic artifact on the anchorage plate.

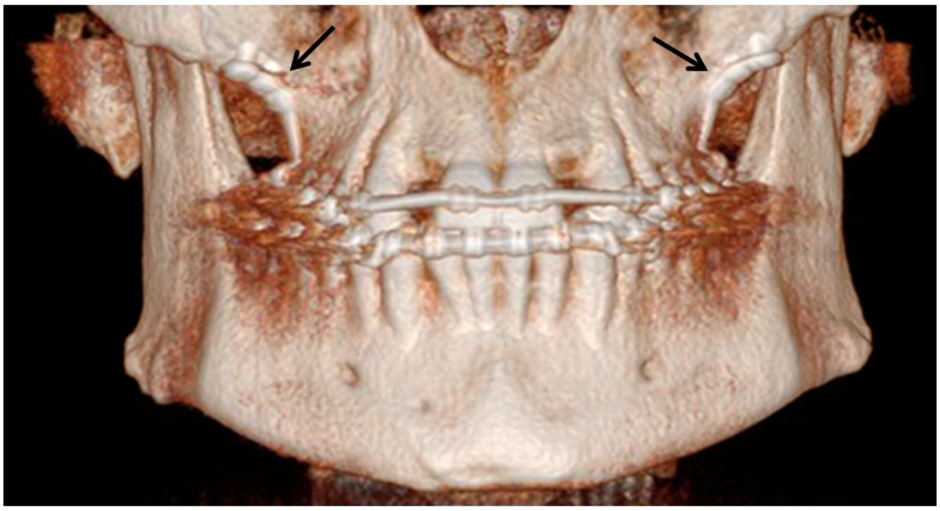

Fig. 45. I-CAT CBCT. 3D reconstruction of maxilla and mandible, anterior view. Black arrows: Orthodontic anchorage plate (Bollard type) without metallic artifact.

Discussion

The reduction of aliasing artifact is related with the improvement of detectors quality [8]. When ring artifact is found the dentist should ask for help the CBCT manufacturing company (importance of after selling service contract) as lost of calibration of CBCT can cause errors in on-screen measurements and further errors in diagnosis and treatment planning.

For beam hardening artifact, it is advisable to reduce the field of view (FOV) [9] to avoid scanning regions susceptible to beam hardening (e.g., metallic restorations, dental implants), which can be achieved by collimation, modification of patient positioning, or separation of the dental arches [3]. Dark spaces around implants are due to beam hardening artifact (Figure 9)and should not be interpreted as peri-implantitis. Diagnosis of peri-implantitis is clinical and could be completed using a periapical conventional intraoral X-ray [10]. The zirconia implants produce more artifacts and its images are more affected by the different protocols than titanium implants [11].

The importance of beam hardening artifact is related to the density of material and may vary from major perturbation of image with subperiosteal implants (Figures 10-13) to no perturbation with metallic orthodontic anchorage (Figures 44, 45). Beam hardening artifacts may vary according to the type and to the alloy material used in manufacturing of osteosynthesis screws. Screws used to fix orbit titanium plate (Figures 28, 29) shows less artifact than screws to fix titanium mesh on frontal bone (Figures 31-33). This may be of importance when checking if screws are not in

contact or damage roots of teeth after trauma or orthognathic surgery. With presence of important beam hardening artifact around screws it becomes impossible to clearly evaluate a close relationship between screws and dental roots.
A check list procedure should be installed in dental practice to avoid unnecessary beam hardening artifacts. Especially, glasses, necklace, removable prostheses, piercings (whose can be removed), earrings, hair clips should be removed before CBCT examination. Hearing aid device could remain in place as it does not artifact the dentomaxillofacial area of interest, and allows the contact with the patient. Moreover, beam hardening artifacts related to hearing aid devices will be visible only in large fields of view in dentomaxillofacial radiology. Dreadlocks clips give beam hardening artifact outside of dentomaxillofacial area, and can stay in place during the scanning.

Finally, when looking at PubMed database the accessibility to open knowledge on technically related CBCT artifacts seems extremely limited with only 4 figures freely accessible; thus the need to share practical knowledge related to CBCT images. The author fully supports values of open science – sharing knowledge has the potential to increase the quality of science system. All images are in CC-BY-SA license and they can be freely reproduced, under condition of citing correctly the source.

- **Acknowledgements:** none
- **Funding sources statement**: this study does not received any funding

- **Competing interests**: Prof R. Olszewski is Editor-in-Chief of Nemesis
- **Ethical approval**: There was no need for ethical committee approval for this study
- **Informed consent**: There was no need for informed consent for this study

Authors contribution:

Author	Contributor role
Olszewski Raphael	Conceptualization, Data curation, Investigation, Methodology, Resources, Validation, Writing original draft preparation, Supervision, Writing review and editing

References

1. Pauwels R, Araki K, Siewerdsen JH, Thongvigitmanee SS. Technical aspects of dental CBCT: state of the art. Dentomaxillofac Radiol 2015;44:20140224.

2. Schulze R, Heil U, Gross D, Bruellmann DD, Dranischnikow E, Schwanecke U, Schoemer E. Artefacts in CBCT: a review. Dentomaxillofac Radiol 2011;40:265-273.

3. Nagarajappa AK, Dwivedi N, Tiwari R. Artifacts: The downturn of CBCT image. J Int Soc Prev Community Dent 2015;5:440-445.

4. Esmaeili F, Johari M, Haddadi P, Vatankhah M. Beam hardening artifacts: Comparison between two cone beam computed tomography scanners. J Dent Res Dent Clin Dent Prospects 2012;6:49–53.

5. Ibraheem I. Reduction of artifacts in dental cone beam CT images to improve the three dimensional image reconstruction. J Biomed Sci Eng 2012;5:409–415.

6. Nabha W, Hong YM, Cho JH, Hwang HS. Assessment of metal artifacts in three-dimensional dental surface models derived by cone-beam computed tomography. Korean J Orthod 2014;44:229–235.

7. Streel R. Oral rehabilitation with implant dentures. Dent News 1987;9:36, 39-41 contd.

8. Xie H, Tang X. Optimization of data acquisition in axial CT under the framework of sampling on lattice for suppression of aliasing artifacts with algorithmic detector interlacing. Med Phys 2017;44:6239-6250.

9. Shokri A, Jamalpour MR, Khavid A, Mohseni Z, Sadeghi M. Effect of exposure parameters of cone beam computed tomography on metal artifact reduction around the dental implants in various bone densities. BMC Med Imaging 2019;19:34.

10. Steiger-Ronay V, Krcmaric Z, Schmidlin PR, Sahrmann P, Wiedemeier DB, Benic GI. Assessment of peri-implant defects at titanium and zirconium dioxide implants by means of periapical radiographs and cone beam computed tomography: An in-vitro examination. Clin Oral Implants Res 2018;29:1195-1201.

11. Vasconcelos TV, Leandro Nascimento EH, Bechara BB, Freitas DQ, Noujeim M. Influence of cone beam Computed Tomography settings on implant artifact production: zirconia and titanium. Int J Oral Maxillofac Implants 2019;34:1114-1120.